



# Direct Vector Control of a DFIG Supplied by an Intelligent SVM Inverter for Wind Turbine System

H. Benbouhenni\* (C.A.), Z. Boudjema\*\* and A. Belaidi\*

**Abstract:** This article presents an improved direct vector command (DVC) based on intelligent space vector modulation (SVM) for a doubly fed induction generator (DFIG) integrated in a wind turbine system (WTS). The major disadvantages that is usually associated with DVC scheme is the power ripples and harmonic current. To overcome this disadvantages an advanced SVM technique based on fuzzy regulator (FSVM) is proposed. The proposed regulator is shown to be able to reduce the active and reactive powers ripples and to improve the performances of the DVC method. Simulation results are shown by using Matlab/Simulink.

**Keywords:** DVC, DFIG, SVM, FSVM, Fuzzy Regulator, Powers Ripples.

## 1 Introduction

THE DFIG is at present the most commonly used in WTSs due to their advantageous qualities of cost, robustness, and performances. In the most WTSs configurations, the stator side is directly connected to the grid and the rotor side is connected to the grid through a back-to-back converter [1, 2]. Many command schemes such as vector command (VC) [3, 4], sliding mode command (SMC) [5, 6], artificial intelligent command (AIC) [7], direct torque command (DTC) [8-10], LQR command of DFIG [11] and direct power command (DPC) [12, 13] have been proposed to command especially active and reactive powers of the DFIG.

Since vector command scheme is employed to command the grid-side converter (GSC) and rotor-side converter (RSC). Controlling the active and reactive energy of DFIG is separately performed by vector command of RSC, thus achieving the regulatory energy factor is possible. However, VC of GSC in addition to supporting the DC link voltage can command the active

energy exchanged between the GSC and the grid [14]. A decoupled command of the stator active and reactive powers has been achieved by regulating the decomposed rotor currents with PI regulators [15]. Since the PWM (pulse width modulation) strategy is usually used in command of machine drive. However, this strategy scheme is the simple one and easy to implement. On the other hand, this strategy gives more THD (total harmonic distortion), and high ripple in torque, flux and powers of the DFIG machine. To overcome the drawbacks of classical PWM strategy, a new modulation strategy for the inverter control was proposed by [16, 17] as space vector modulation to command active and reactive powers. However, this technique gives 15% more voltage output compared to the classical PWM technique. On the other hand, the SVM technique is complex command and need to calculate the sector and angle. In this article, we propose a new SVM strategy based on the calculation of minimum and maximum of three-phase voltage. The advantages of the proposed SVM strategy is not needed to calculate the angle and sector, easy to implement, simple scheme and gives minimum THD compared to PWM modulation.

On the other hand, the essential drawbacks of SVM strategy using hysteresis controllers are the variable switching frequency and high ripples. To avoid these problems of the SVM technique, a new SVM technique has been proposed in this article based on fuzzy logic (FSVM).

In our paper, three different DVC command schemes

Iranian Journal of Electrical and Electronic Engineering, 2019.

Paper first received 24 February 2018 and accepted 30 July 2018.

\* The authors are with the Ecole Nationale Polytechnique d'Oran Maurice Audin, Oran, Algeria.

E-mails: [habib0264@gmail.com](mailto:habib0264@gmail.com) and [belaidiaek@gmail.com](mailto:belaidiaek@gmail.com).

\*\* The author is with the Electrical Engineering Department, Faculty of Technology, Hassiba Benbouali University, Chlef, Algeria.

E-mail: [boudjema1983@yahoo.fr](mailto:boudjema1983@yahoo.fr).

Corresponding Author: H. Benbouhenni.

will be compared with each other. These schemes are DVC command using classical PWM technique, DVC using SVM technique and DVC using FSVM strategy. The proposed commands schemes are described clearly and simulation results are reported to demonstrate its effectiveness. The used command schemes are implemented in Matlab.

### 2 The Model of DFIG

The model of the DFIG is same as the cage induction machine. The application of Park model of the DFIG permits to write the dynamic voltages and fluxes equations in dq reference frame are given by the following equations [18, 19]:

$$\begin{cases} V_{ds} = R_s I_{ds} + \frac{d}{dt} \psi_{ds} - \omega_s \psi_{qs} \\ V_{qs} = R_s I_{qs} + \frac{d}{dt} \psi_{qs} + \omega_s \psi_{ds} \\ V_{dr} = R_r I_{dr} + \frac{d}{dt} \psi_{dr} - \omega_r \psi_{qr} \\ V_{qr} = R_r I_{qr} + \frac{d}{dt} \psi_{qr} + \omega_r \psi_{dr} \end{cases} \quad (1)$$

Rotor and stator fluxes:

$$\begin{cases} \psi_{ds} = L_s I_{ds} + M I_{dr} \\ \psi_{qs} = L_s I_{qs} + M I_{qr} \\ \psi_{dr} = L_r I_{dr} + M I_{ds} \\ \psi_{qr} = L_r I_{qr} + M I_{qs} \end{cases} \quad (2)$$

The torque is done as:

$$T_e = pM (I_{dr} \cdot I_{qs} - I_{qr} \cdot I_{ds}) \quad (3)$$

and its associated motion equation is:

$$T_e = T_r + J \cdot \frac{d\Omega}{dt} + f \cdot \Omega \quad (4)$$

where  $I_{dr}$ ,  $I_{qr}$  are rotor current components,  $V_{ds}$ ,  $V_{qs}$  are stator voltage components,  $V_{dr}$ ,  $V_{qr}$  are rotor voltage components,  $R_s$  and  $R_r$  are stator and rotor resistances,  $L_s$  and  $L_r$  are stator and rotor inductances,  $M$  is mutual inductance,  $T_e$  is the torque,  $T_r$  is the load torque,  $\Omega$  is

the mechanical rotor speed,  $J$  is the inertia,  $f$  is the viscous friction coefficient and  $p$  is the number of pole pairs.

The stator area  $P_s$  and  $Q_s$  powers are defined as:

$$\begin{cases} P_s = \frac{3}{2} (V_{ds} I_{ds} + V_{qs} I_{qs}) \\ Q_s = \frac{3}{2} (V_{qs} I_{ds} - V_{ds} I_{qs}) \end{cases} \quad (5)$$

### 3 DVC Command

In this work, the DFIG model can be described by the following state equations in the synchronous orientation frame whose axis d is aligned with the stator flux vector.

$$\psi_{ds} = \psi_s \quad \text{and} \quad \psi_{qs} = 0 \quad (6)$$

On the other hand, by neglecting  $R_s$  the stator voltage can be expressed by:

$$\begin{cases} V_{ds} = 0 \\ V_{qs} = \omega_s \psi_s \end{cases} \quad (7)$$

$$\begin{cases} I_{ds} = -\frac{M}{L_s} I_{dr} + \frac{\psi_s}{L_s} \\ I_{qs} = -\frac{M}{L_s} I_{qr} \end{cases} \quad (8)$$

The active and reactive powers consequently given by the following expression:

$$\begin{cases} P_s = -\frac{3}{2} \frac{\omega_s \psi_s M}{L_s} I_{qr} \\ Q_s = -\frac{3}{2} \left( \frac{\omega_s \psi_s M}{L_s} I_{dr} - \frac{\omega_s \psi_s^2}{L_s} \right) \end{cases} \quad (9)$$

The torque can then be expressed by [20]:

$$T_e = -\frac{3}{2} p \frac{M}{L_s} I_{qr} \psi_{ds} \quad (10)$$

Fig. 1 represents the DVC command technique of DFIG driven by a classical inverter using PWM inverter.

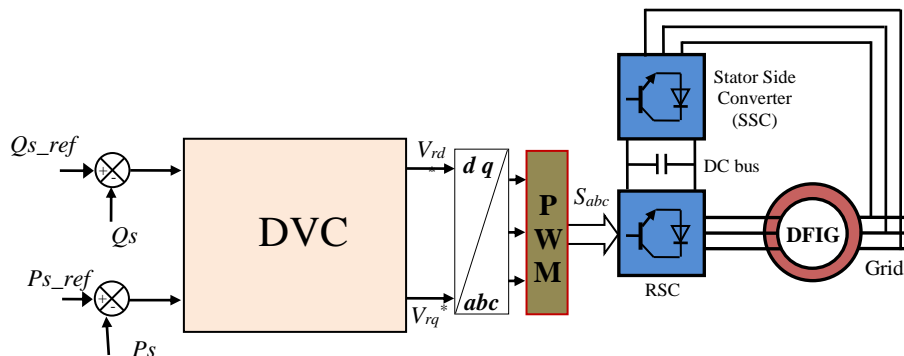


Fig. 1 DVC method block with PWM inverter.

The internal structure of DVC method is shown in Fig. 2.

The PI regulators terms are calculated with a pole compensation strategy [21]. The time response of the regulated system will be fixed at 10 ms. This value is adequate for our application and a lower value might involve transient with important overshoot. The calculated terms are:

$$K_i = 1000 \frac{L_s R_r}{M V_s} \tag{11}$$

$$K_p = 1000 \frac{L_s R_r \sigma}{M V_s} \tag{12}$$

The terms  $K_i$  and  $K_p$  represent respectively the integral and proportional gains of PI regulator.

On the other hand, the DVC scheme of DFIG is the simple command method and easy to implement. Like

an every scheme method has some advantages and disadvantages. The basic disadvantages of DVC scheme using PWM inverter are the variable switching frequency, the stator reactive and stator active powers ripples. In the aim to improve the performance of the electrical drives based on classical DVC command, Space Vector Modulation (SVM) inverter and fuzzy logic space vector modulation inverter (FSVM) to reduce the reactive, active powers ripple and minimize the THD value of current ( $I_{as}$ ).

Fig. 3 shows the schematic block of a DVC method with FSVM technique. The principal of the DVC command using FSVM technique is similar to classical DVC command. However, the PWM inverter is replaced by FSVM inverter. This strategy technique based on fuzzy classification has the advantage of simplicity and easy to implement.

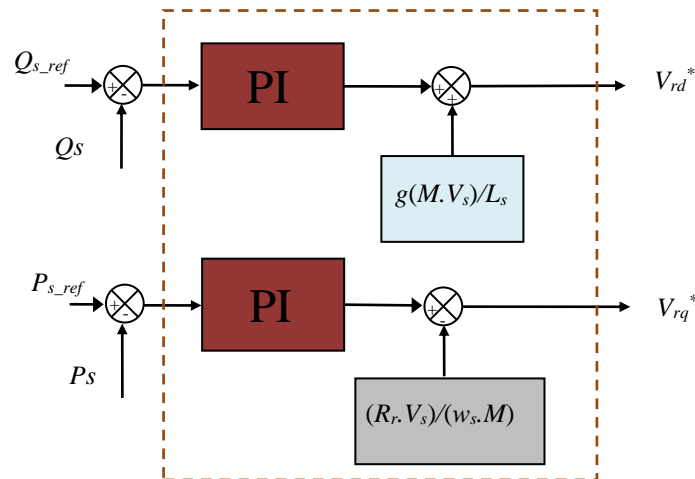


Fig. 2 Structure of DVC scheme.

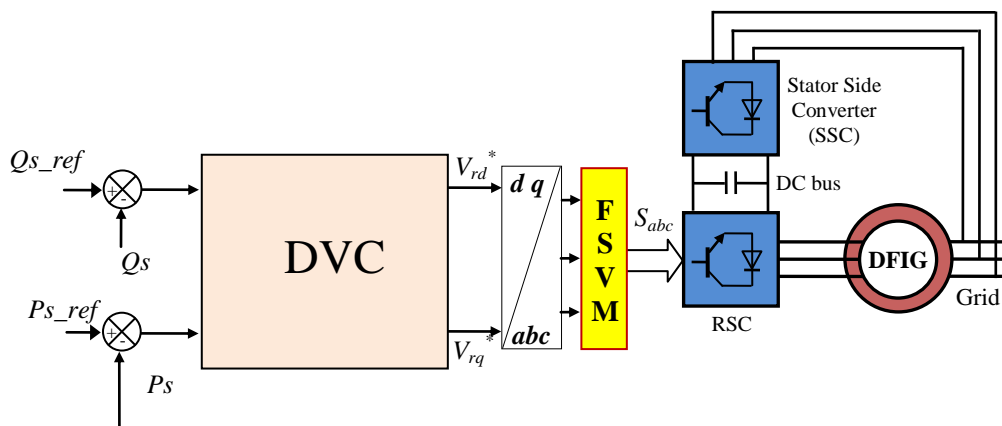


Fig. 3 DVC method block with FSVM inverter.

### 4 Intelligent Space Vector Modulation

#### 4.1 SVM Strategy

The SVM technique considers this contact of the phase and reduced the ripple content of the three-phase isolated neutral load as shown in Fig. 4 [22]. The SVM method is recently showing popularity for inverter applications.

The three phases sinusoidal and balance voltages given by the equations as follows:

$$\begin{cases} V_{An} = V_m \cos(\omega t) \\ V_{Bn} = V_m \cos(\omega t + \frac{2\pi}{3}) \\ V_{Cn} = V_m \cos(\omega t + \frac{4\pi}{3}) \end{cases} \quad (13)$$

$$V^- = \frac{2}{3} [V_{An} + aV_{Bn} + a^2V_{Cn}] \quad (14)$$

In this article, we propose a simple technique of SVM based on following steps:

- Calculate the *minimum* voltages,  $\min(V_{Ao}, V_{Bo}, V_{Co})$ ,
- Calculate the *maximum* voltages,  $\max(V_{Ao}, V_{Bo}, V_{Co})$ ,
- Find the switching states.

The SVM inverter block represents the two-level inverter model as shown in Fig. 5. The energy converter has been implemented in terms of the switching function  $g_i$  connected with each energy switch. The switching function  $g_i$  of a given energy switching can assume either 1 or 0 according to its conducting state. Since two energy switches of the similar leg cannot be on at the same time, the switching function of the phase ‘A’ for example, is distinct as:

$$g_a + g_{a'} = 1 \quad (15)$$

The principle of SVM method is that the command

electrical energy vector is approximately calculated by using three adjacent vectors [23]. However, this modulation technique is detailed in [24-26].

The output phase voltages, in terms of the switching functions are:

$$\begin{bmatrix} V_{An} \\ V_{Bn} \\ V_{Cn} \end{bmatrix} = \frac{E}{3} \begin{bmatrix} 2 & -1 & -1 \\ -1 & 2 & -1 \\ -1 & -1 & 2 \end{bmatrix} \begin{bmatrix} g_A \\ g_B \\ g_C \end{bmatrix} \quad (16)$$

#### 4.2 Fuzzy Space Vector Modulation

In order to improve the two-level DVC performances, a complimentary use of the fuzzy regulator (FR) is proposed. The principle of Fuzzy Space Vector Modulation (FSVM) is similar to traditional SVM. The difference is using FRs to replace the hysteresis comparators. As shown in Fig. 6.

Fuzzy logic (FL) is recently getting increasing emphasis in drive command applications. The main preference of the FL is that is easy to implement the command that it has the ability of generalization [27]. The block diagram of FR based hysteresis comparator is shown in Fig. 6. The FR rules are written by absorbing the performance of the hysteresis comparators.

The membership function definition for the input changes “Error in comparators hysteresis” and “Change in Error of comparators hysteresis” is given by Fig. 8.

The FL rules for the proposed system are given in Table 1 [28, 29]. We use the next designations for membership functions:

- NB : Negative Big
- NS : Negative Small
- PB : Positive Big
- PM : Positive Middle.
- NM : Negative Middle
- PS : Positive Small
- EZ : Equal Zero

Table 2 shows the parameters of FR.

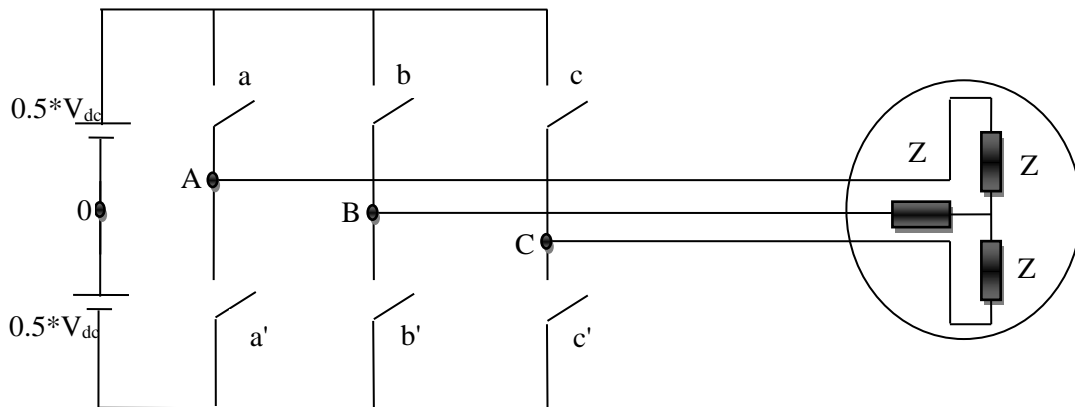


Fig. 4 Voltage source inverter type three phase.

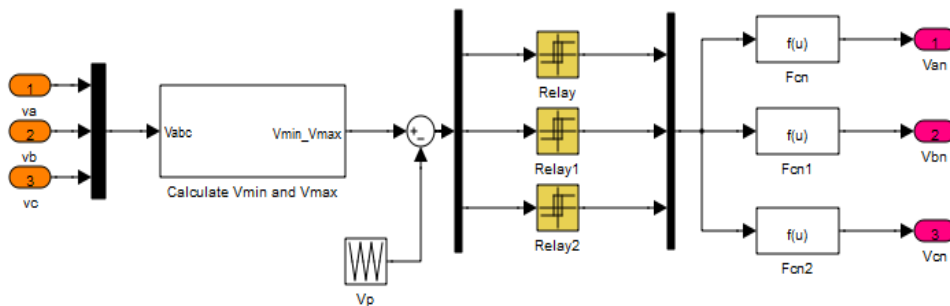


Fig. 5 Simulation block of proposed SVM technique.

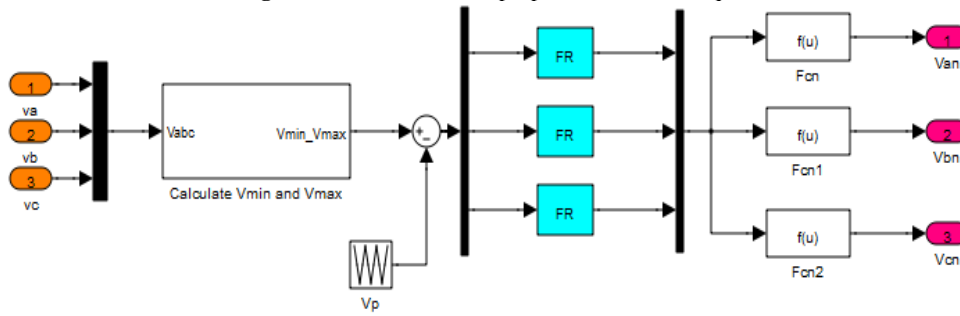


Fig. 6 SVM method with FR.

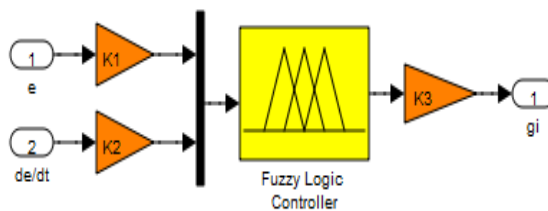


Fig. 7 Fuzzy command of comparators hysteresis.

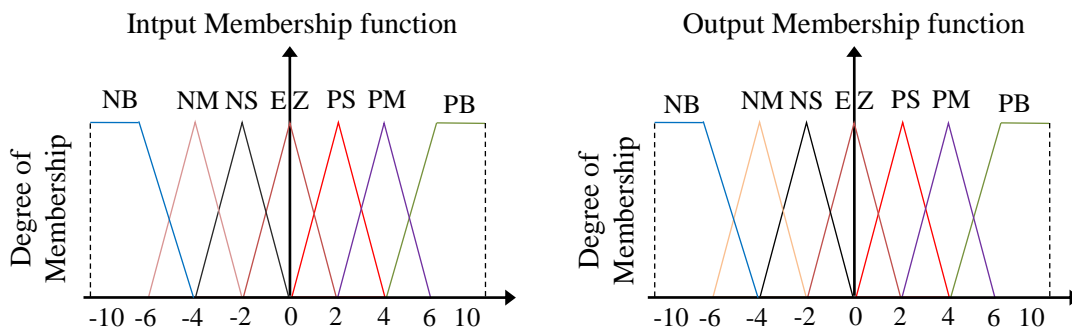


Fig. 8 FR sets and its memberships functions.

Table 1 FL rules of hysteresis comparators.

$\begin{matrix} e \\ \Delta e \end{matrix}$	NB	NM	NS	EZ	PS	PM	PB
NB	NB	NB	NB	NB	NM	NS	EZ
NM	NB	NB	NB	NM	NS	EZ	PS
NS	NB	NB	NM	NS	EZ	PS	PM
EZ	NB	NM	NS	EZ	PS	PM	PB
PS	NM	NS	EZ	PS	PM	PB	PB
PM	NS	EZ	PS	PM	PB	PB	PB
PB	EZ	PS	PM	PB	PB	PB	PB

$e = V_2 - V_p, \Delta e = d(V_2 - V_p)/dt$

Table 2 Parameters of FR.

Fis Type	Mamdani
And Method	Min
Or Method	Max
Implication	Min
Aggregation	Max
Defuzzification	Centroid

### 5 Simulations Results

The DVC scheme of a DFIG is implemented with simulation tools of MATLAB. The DFIG (1.5 MW) attached to a 398 V/50 Hz grid. Parameters of the DFIG are given in Table 3 [30, 31]. The both command strategies DVC using PWM, DVC using SVM and DVC using FSVM technique are simulated and compared regarding reference tracking, current harmonics distortion, and robustness against DFIG parameter variations.

#### 5.1 Reference Tracking Test

Figs. 9-19 show the obtained simulation results. As it is shown in Figs. 9-12, for the three DVC command

strategies, the reactive, electromagnetic torque and stator active powers tracks almost perfectly their references values. Moreover, the DVC command using FSVM strategy reduced the powers ripples and torque ripple compared to the DVC command using PWM and SVM technique (see Figs. 13-16). On the other hand, Figs. 17-19 show the THD of stator current of the doubly fed induction generator obtained using Fast Fourier Transform (FFT) method for both DVC command schemes. It can be clearly observed that the THD value is minimized for DVC using FSVM technique (THD = 0.09%) when compared to DVC command using PWM (THD = 1.22%) and DVC command using SVM technique (THD = 1.19%).

**Table 3** The DFIG parameters.

Parameters	Rated Value	Unity
Nominal power	1.5	MW
Stator voltage	398	V
Stator frequency	50	Hz
Number of pairs poles	2	
Stator resistance	0.012	$\Omega$
Rotor resistance	0.021	$\Omega$
Stator inductance	0.0137	H
Rotor inductance	0.0136	H
Mutual inductance	0.0135	H
Inertia	1000	Kg.m <sup>2</sup>
Viscous friction	0.0024	Nm/s

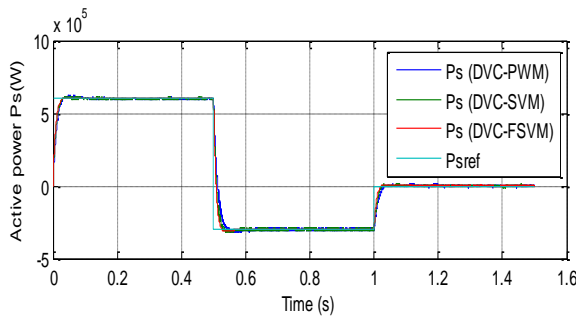


**Fig. 9** Active power (Reference tracking test).

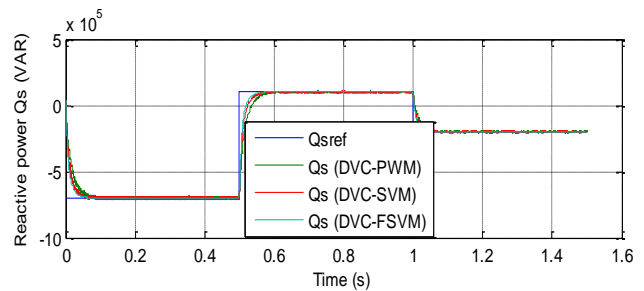


**Fig. 10** Reactive power (Reference tracking test).

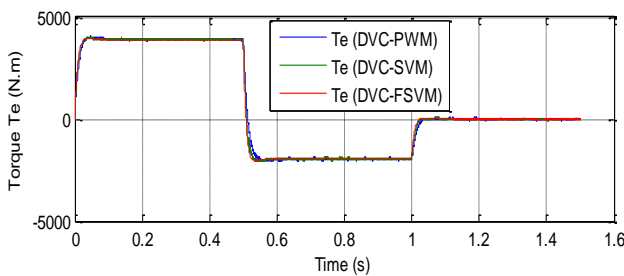


**Fig. 11** Torque (Reference tracking test).

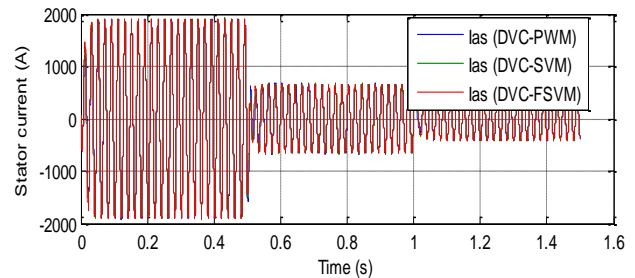


**Fig. 12** Stator current (Reference tracking test).

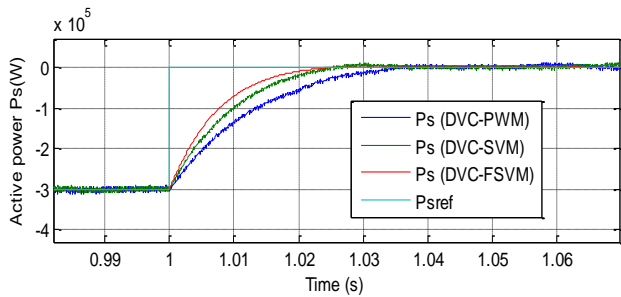


Fig. 13 Zoom in the active power (Reference tracking test).

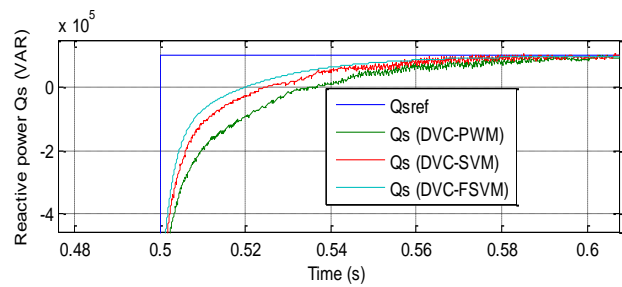


Fig. 14 Zoom in the reactive power (Reference tracking test).

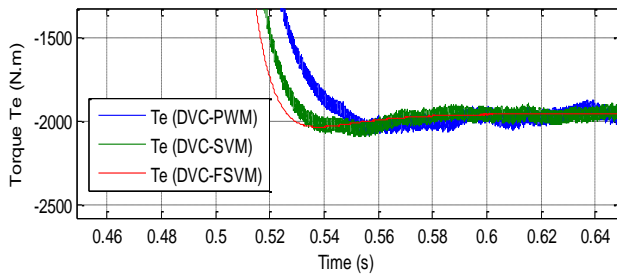


Fig. 15 Zoom in the torque (Reference tracking test).

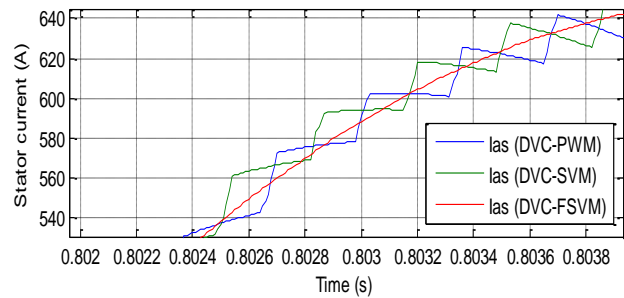


Fig. 16 Zoom in the stator current (Reference tracking test).

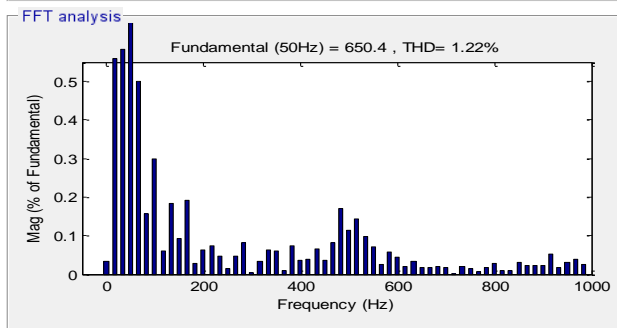
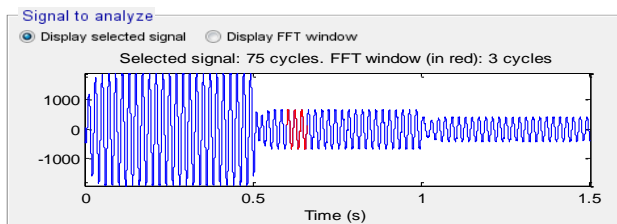


Fig. 17 THD of one phase stator current for DVC-PWM (Reference tracking test).

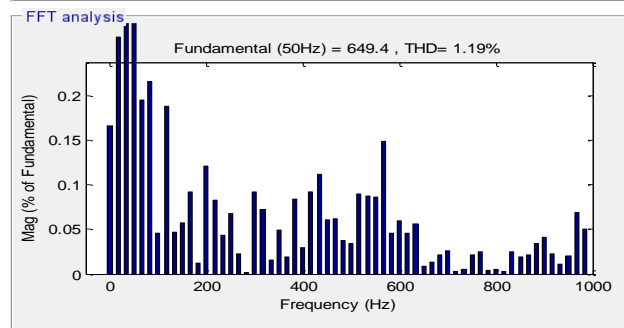
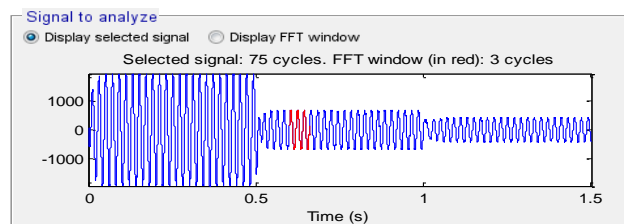


Fig. 18 THD of one phase stator current for DVC-SVM (Reference tracking test).

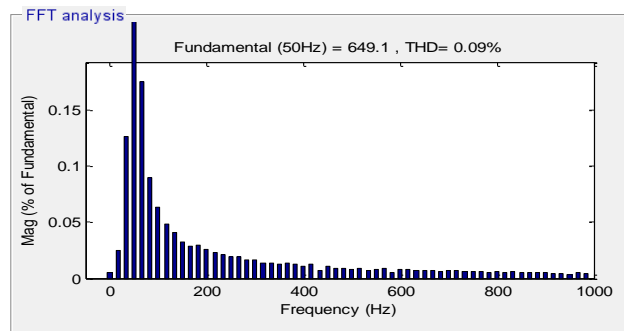
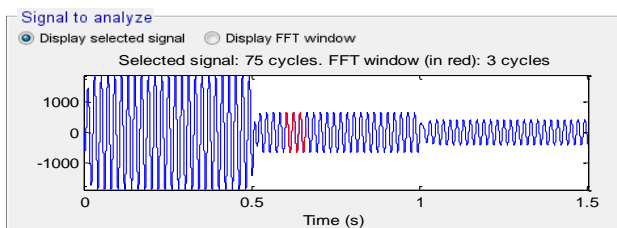


Fig. 19 THD of one phase stator current for DVC-FSVM (Reference tracking test).



**5.2 Robustness Test**

In order to study the robustness of the proposed command schemes, the nominal value of the  $R_r$  and  $R_s$  is multiplied by 2, the values of inductances  $L_s$ ,  $M$ , and  $L_r$  are multiplied by 0.5. Simulation results are presented in Figs. 20-30. As it is shown by these figures, these variations present an apparent effect on the active, reactive powers, and electromagnetic torque curves and that the effect appears more significant for the DVC using PWM technique compared to DVC using SVM

strategy (see Figs. 24-27).

On the other hand, this variation does not effect on the DVC using FSVM technique. However, the THD value of stator current in the DVC using FSVM technique has been reduced significantly (see Figs. 28-30). Table 4 shows the comparative analysis of THD value. Thus it can be concluded that the proposed DVC using FSVM inverter is more robust than the DVC using PWM and SVM technique.

**Table 4** Comparative analysis of THD value.

	THD [%]		
	DVC-PWM	DVC-SVM	DVC-FSVM
Stator Current	6.92	6.86	0.19

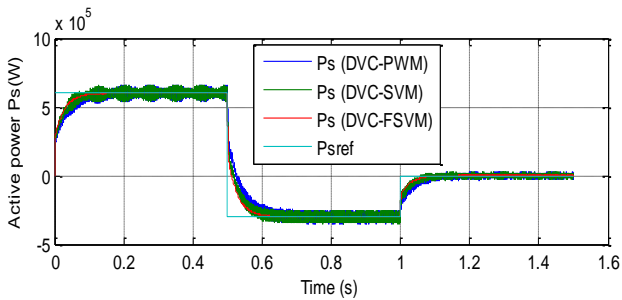


**Fig. 20** Active power (robustness test).

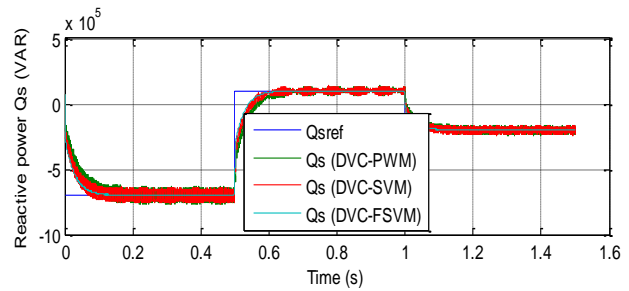


**Fig. 21** Reactive power (robustness test).

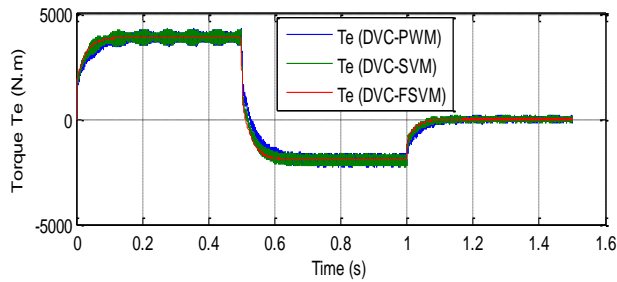


**Fig. 22** Torque (robustness test).

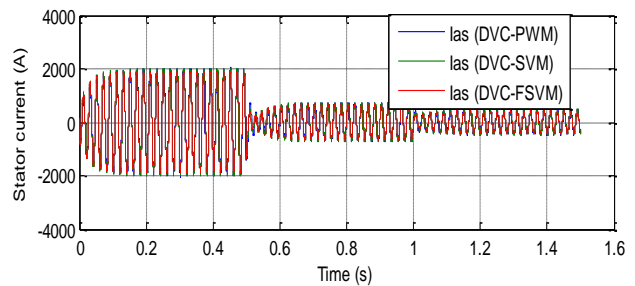


**Fig. 23** Stator current (robustness test).

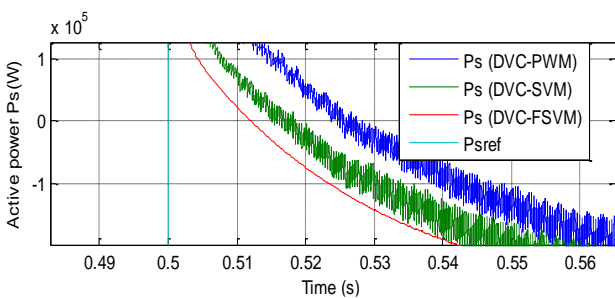


**Fig. 24** Zoom in the active power (robustness test).

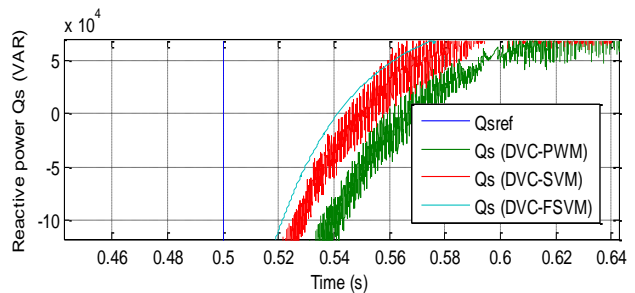


**Fig. 25** Zoom in the reactive power (robustness test).

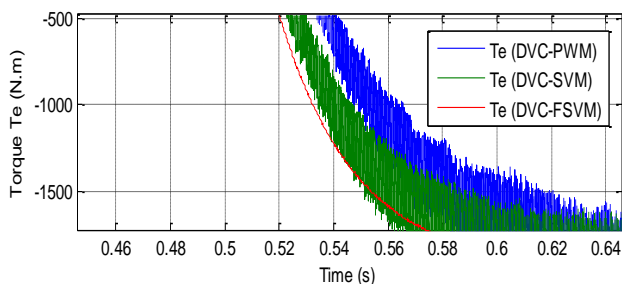


**Fig. 26** Zoom in the torque (robustness test).

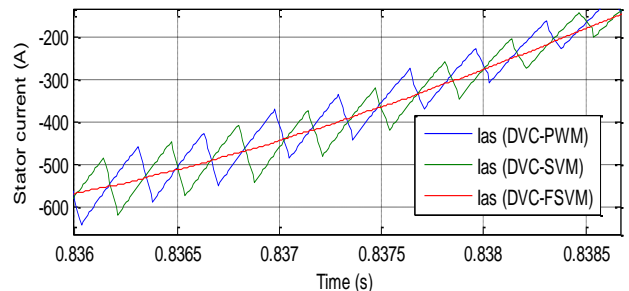


**Fig. 27** Zoom in the stator current (robustness test).



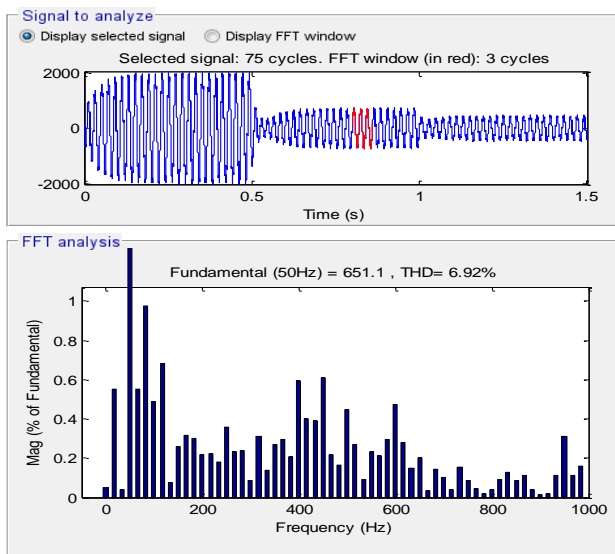


Fig. 28 THD of one phase stator current for DVC-PWM (robustness test).

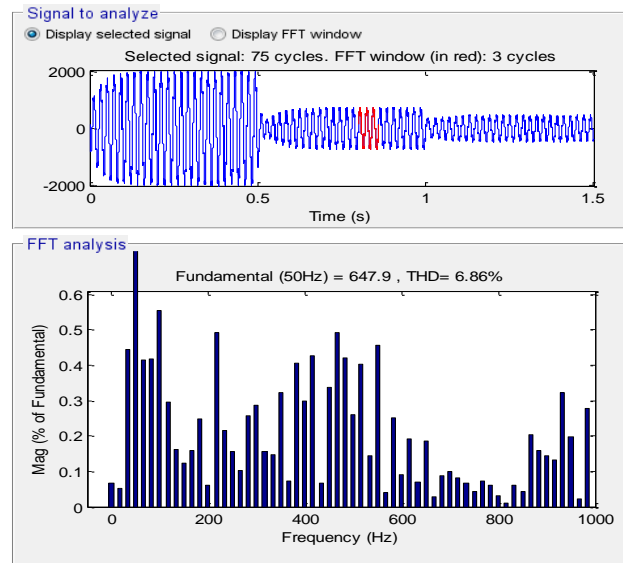


Fig. 29 THD of one phase stator current for DVC-SVM (robustness test).

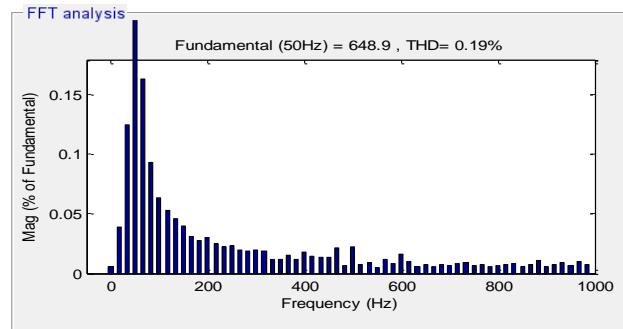
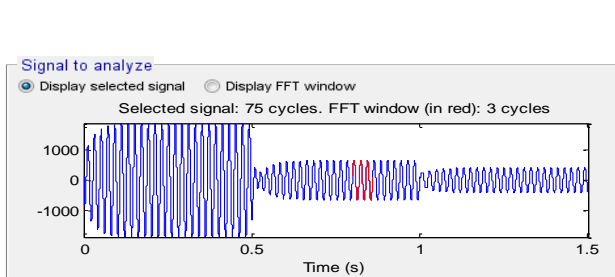


Fig. 30 THD of one phase stator current for DVC-FSVM (Reference tracking test).

## 6 Conclusion

This article presents a novel DVC scheme of a DFIG using a new modulation technique based on SVM and fuzzy logic compared with the classical PWM and SVM strategies. With results obtained from the simulation, it was clear that for the same operation conditions, the DVC scheme with FSVM technique presents good performance compared to the DVC one using SVM and PWM strategies and that was clear in the THD of current which the use of the FSVM minimize the THD more and more than the classical PWM and SVM strategy.

## References

[1] Y. Bekakra and D. Ben Attous, "Comparison study between SVM and PWM inverter in sliding mode control of active and reactive power control of a DFIG for variable speed wind energy," *International Journal of Renewable Energy Research*, Vol. 2, No. 3, pp. 471–476, 2012.

[2] M. Hosseinabadi and H. Rastegar, "DFIG based wind turbines behavior improvement during wind variations using fractional order control systems," *Iranian Journal of Electrical and Electronic Engineering*, Vol. 10, No. 4, pp. 314–323, 2014.

[3] A. Medjber, Moualdia, A. Mellit and M. A. Guessoum, "Comparative study between direct and indirect vector control applied to a wind turbine equipped with a double-fed asynchronous machine article," *International Journal of Renewable Energy Research*, Vol. 3, No. 1, pp. 88–93, 2013.

[4] B. Hamane, M. L. Doumbia, M. Bouhamida, A. Draou, H. Chaoui, and M. Benghanem, "Comparative study of PI, RST, sliding mode and fuzzy supervisory controllers for DFIG based wind energy conversion system," *International Journal of Renewable Energy Research*, Vol. 5, No. 4, pp. 1174–1184, 2015.

- [5] A. Yahdou, B. Hemici, and Z. Boudjema, "Second order sliding mode control of a dual-rotor wind turbine system by employing a matrix converter," *Journal of Electrical Engineering*, Vol. 16, No. 4, pp. 1–11, 2016.
- [6] Z. Boudjema, A. Meroufel, Y. Djerriri, and E. Bounadja, "Fuzzy sliding mode control of a doubly fed induction generator for wind energy conversion," *Carpathian Journal of Electronic and Computer Engineering*, Vol. 6, No. 2, pp. 7–14, 2013.
- [7] A. Bakouri, H. Mahmoudi, and A. Abbou, "Intelligent control for doubly fed induction generator connected to the electrical network," *International Journal of Power Electronics and Drive System*, Vol. 7, No. 3, pp. 688–700, 2016.
- [8] S. Massoum, A. Meroufel, A. Massoum, and P. Wira, "A direct power control of the doubly-fed induction generator based on the SVM strategy," *Elektrotehniski Vestnik*, Vol. 45, No. 5, pp. 235–240, 2017.
- [9] Z. Boudjema, R. Taleb, Y. Djerriri, and A. Yahdou, "A novel direct torque control using second order continuous sliding mode of a doubly fed induction generator for a wind energy conversion system," *Turkish Journal of Electrical Engineering & Computer Sciences*, Vol. 25, pp. 965–975, 2017.
- [10] Y. S. Rao and A. J. Laxmi, "Direct torque control of doubly fed induction generator based wind turbine under voltage dips," *International Journal of Advances in Engineering & Technology*, Vol. 3, No. 2, pp. 711–720, 2012.
- [11] A. Khajah and R. Ghazi, "GA-based optimal LQR controller to improve LVRT capability of DFIG wind turbine," *Iranian Journal of Electrical and Electronic Engineering*, Vol. 9, No. 3, pp. 167–176, 2013.
- [12] S. M. Tavakoli, Pourmina and M. R. Zolghadri, "Comparison between different DPC methods applied to DFIG wind turbines," *International Journal of Renewable Energy Research*, Vol. 3, No. 2, pp. 446–452, 2013.
- [13] F. Amrane and A. Chaiba, "A novel direct power control for grid-connected doubly fed induction generator based on hybrid artificial intelligent control with space vector modulation," *Rev. Roum. Sci. Techn.-Electrotechn. Et Energ*, Vol. 61, No. 3, pp. 263–268, 2016.
- [14] M. J. Abbasi and H. Yaghobi, "Loss of excitation detection in doubly fed induction generator by voltage and reactive power rate," *Iranian Journal of Electrical and Electronic Engineering*, Vol. 12, No. 4, pp. 270–280, 2016.
- [15] E. G. Shehata, "Sliding mode direct power control of RSC for DFIGs driven by variable speed wind turbines," *Alexandria Engineering Journal*, Vol. 54, pp. 1067–1075, 2015.
- [16] V. Meenakshi, G. D. Anbarasi, and J. S. Paramasivam, "Space vector modulation technique applied to doubly fed induction generator," *Indian Journal of Science and Technology*, Vol. 8, pp. 1–8, 2015.
- [17] B. Belkacem, L. A. Koridak, and M. Rahli, "Comparative study between SPWM and SVPWM control of a three level voltage inverter dedicated to a variable speed wind turbine," *Journal of Power Technologies*, Vol. 97, No. 3, pp. 190–200, 2017.
- [18] F. Senani, A. Rahab, and H. Benalla, "Modeling and control of active and reactive powers of wind energy conversion system in variable speed based on DFIG," *Revue des Energies Renouvelables*, Vol. 18, No. 4, pp. 643–655, 2015.
- [19] D. Phan and S. Yamamoto, "Maximum energy output of a DFIG wind turbine using an improved MPPT-curve method," *Energies*, Vol. 8, pp. 11718–11736, 2015.
- [20] K. Boulaam and A. Boukhelifa, "Output power control of a variable wind energy conversion system," *Rev. Roum. Sci. Techn.-Electrotechn. Et Energ*, Vol. 62, No. 2, pp. 197–202, 2017.
- [21] Y. Bekakra and D. B. Attous, "DFIG sliding mode control driven by wind turbine with using a SVM inverter for improve the quality of energy injected into the electrical grid," *ECTI Transactions on Electrical Engineering, Electronics, and Communications*, Vol. 11, No. 1, pp. 63–75, 2013.
- [22] A. K. Bilhan and E. Akbal, "Modeling and simulation of two-level space vector PWM inverter using photovoltaic cells as DC source," *International Journal of Electronics, Mechanical and Mechatronics Engineering*, Vol. 2, No. 4, pp. 311–317, 2016.
- [23] A. Idir and M. Kidouche, "Direct torque control of three phase induction motor drive using fuzzy logic controllers for low torque ripple," in *Proceedings Engineering & Technology*, Vol. 2, pp. 78–83, 2013.
- [24] M. Gaballah and M. El-bardini, "Low cost digital signal generation for driving space vector PWM inverter," *Ain Shams Engineering Journal*, Vol. 4, pp. 763–774, 2013.
- [25] M. A. Moghadam, R. Noroozian, and S. Jalilzadeh, "Modeling, simulation and control of matrix converter for variable speed wind turbine system," *Iranian Journal of Electrical and Electronic Engineering*, Vol. 11, No. 3, pp. 265–275, 2015.

- [26] A. Chikhi, "Direct torque control of induction motor based on space vector modulation using a fuzzy logic speed controller," *Jordan Journal of Mechanical and Industrial Engineering*, Vol. 8, No. 3, pp. 169–176, 2014.
- [27] Z. Boudjema, A. Meroufel, E. Bounadja, and Y. Djerriri, "Nonlinear control of a doubly fed induction generator supplied by a matrix converter for wind energy conversion systems," *Journal of Electrical Engineering*, Vol. 14, No. 2, pp. 60–68, 2014.
- [28] H. Benbouhenni, "36 Sectors DTC based on fuzzy logic of sensorless induction motor drives," *Research & Reviews: Journal of Engineering and Technology*. Vol. 7, No. 1, pp. 24–32, 2018.
- [29] H. Benbouhenni and Z. Boudjema, "Speed regulator and hysteresis based on artificial intelligence techniques of three-level DTC for induction motor," *Acta Electrotechnica et Informatica*, Vol. 17, No. 4, pp. 50–56, 2017.
- [30] D. Youcef, A. Meroufel, and A. Massoum, "Direct power control based artificial neural network of doubly fed induction generator for wind energy conversion systems," *Rev. Roum. Sci. Techn.-Electrotechn. Et Energ.*, Vol. 54, No.1, pp. 1–22, 2009.
- [31] A. Yahdou, "Commande hybride par mode glissant d'ordre 2 d'un système éolien à double rotor," *Thèse de Doctorat en Sciences*, Ecole Nationale Polytechnique d'Alger, Algeria, 2017.



**H. Benbouhenni** was born in chlef, Algeria. He is a Ph.D. student in the Department of Electrical Engineering at the ENPO-MA, Oran, Algeria. He received a M.A. degree in Automatic and Informatique Industrial in 2017. His research activities include the application of robust control in the wind turbine power systems.



**Z. Boudjema** was born in Algeria in 1983. He is Teacher in university of chlef, Algeria. He received a M.S. degree in electrical engineering from ENP of Oran, Algeria in 2010. He received a Ph.D. in Electrical Engineering from University of Sidi Belabes, Algeria, in 2015. His research activities include the study and application of robust control in the wind-solar power systems.



**A. BELAIDI** is Professor at the National Polytechnic High School - Maurice Audin in Oran. He obtained his Ph.D. in Physics at the University Of East Anglia - UK in 1980. His current fields of interest are nanotechnology, robotics and artificial intelligence.



© 2019 by the authors. Licensee IUST, Tehran, Iran. This article is an open access article distributed under the terms and conditions of the Creative Commons Attribution-NonCommercial 4.0 International (CC BY-NC 4.0) license (<https://creativecommons.org/licenses/by-nc/4.0/>).